Social Influence to Movement Affects Disease Spread in Animal Groups

Jacob Davidson[1], Angela Albi[1], Nivida Thomas[1], sandra.ann.binning[1], and Allison Shaw[1]

[1]Affiliation not available

January 23, 2019

January 23, 2019

Abstract

Parasites have a large impact on a host's life-history evolution, individual behavior, and population dynamics. Recent models have suggested migratory recovery as a strategy to reduce disease prevalence, and experimental work has shown that diseased fish prefer water temperatures that facilitate recovery and lower transmission rates. However, current models ignore the behavioral coupling between social spread of disease, and social influence to movement. We form a model which couples disease transmission with a social influence to movement decisions, and perform simulations to ask how environmental factors and transmission rates influence transient group movement and disease prevalence. The model represents movement between two habitats. The 'breeding' habitat has higher disease transmission rates, but is preferred by healthy individuals because it allows for breeding. The 'recovery' habitat is preferred by diseased individuals because it has low transmission and high recovery rates, but does not allow breeding. An individual's preferred location depends on its disease state and on the motion of others around them via a social network. The model demonstrates that social influence to movement can dramatically change the prevalence of disease as well as the movement dynamics of a group. Current work seeks to test model predictions using experiments with stickleback fish and common species of ectoparasites.

Introduction

Living in groups has both pros and cons. It is normally advantageous in terms of enhanced abilities for predator detection and for finding food. However, an important negative consequence is that the continuous close proximity to group mates can facilitate the spread of disease. The mechanism of "migratory escape" may have evolved to mitigate spread of disease, if individuals move from a high-risk to a low-risk environment in terms of infection spread (Hall et al., 2014; Johns and Shaw, 2015). For instance, seasonal movement between high infection risk, low altitude winter grounds and low infection risk, high altitude summer grounds allows red deer, Cervus elaphus, to reduce their exposure to Ixodes ricinus ticks (Qviller et al., 2013; Mysterud et al., 2015). Further theoretical and empirical work has suggested that "migratory recovery", where movement between environmentally distinct habitats leads to recovery from infection, could be an additional mechanism to reduce overall disease prevalence in a population (Shaw and Binning, 2016; Daversa et al., 2018), and that the spatial distribution of hosts during transient phases influences disease spread (Daversa et al., 2017). Other work has shown that individual location preferences change with disease state (Mohammed et al., 2016). For example, infected individuals may move to warmer habitats that

cause an increase in their surface or core body temperature to the detriment of the parasite, a phenomenon known as "behavioral fever" (Covert and Reynolds, 1977; Kluger et al., 1975; Rakus et al., 2017; Reynolds et al., 1976; Satinoff et al., 1976; Moyer and Wagenbach, 1995). This strategy is particularly effective in ectotherms, which rely on their external environment to regulate internal temperature (Rakus et al., 2017). Such preferences could facilitate movement decisions that aid in the recovery of infected individuals, and lower overall disease prevalence.

The mechanisms of migratory escape, migratory recovery, and behavioral fever involve a sort of "spatial escape", where individuals move to an area that facilitates recovery. However, even though individuals may have their own location preferences, migratory movement decisions are often made in a group setting (Berdahl et al., 2018). Group movement decisions emerge as a result of both social and non-social information use (Pérez-Escudero and de Polavieja, 2011). Models have suggested that only a small number of leaders are needed to change the direction of the whole group (Guttal and Couzin, 2010; Torney et al., 2010; Pais and Leonard, 2014). When preferences are conflicting, the group may compromise or split, depending on the number of individuals and the degree of disagreement (Couzin et al., 2005b; Strandburg-Peshkin et al., 2015).

There are there two ways that movement can affect disease prevalence. The first is moving to an area with higher recovery rates, or escaping an area with high disease transfer rates. The second is escaping from other diseased individuals in the population, who harbor the disease and may transfer it. Group fission/fusion may a key mechanism to balance the trade-off between the benefits of staying together as a group, and the costs due to increased disease transfer.

It is not known how social influence to movement affects the coupling of disease spread and migratory movement. For example, in what conditions will an increase in epidemic spread be caused by an over-reliance on social movement cues? Does the use of social and non-social information depend on disease state? How do individuals balance the trade-off between the benefits of staying in a group, and the costs associated with increased disease transfer?

To address these questions we form a model that couples disease transmission to movement decisions. The model represents movement between two habitats: healthy individuals prefer the 'breeding' habitat, while diseased individuals prefer the 'recovery' habitat. An individual's movement depends both on its disease state, as well on the motion of others around them via a social network. We model disease transfer by using a network version of SIS model, and defining transfer rates depending on distance between individuals. We use the model to ask how social influence to movement affects disease prevalence, depending on the disease transfer and recovery rates in the environment.

We then investigate how a group may mitigate social spread of disease, by considering that healthy individuals can detect diseased individuals, and that adjust their social movement based on the observed disease state of others. We ask what conditions [motion rules?] predict an increase in disease prevalence, versus what is necessary to lead to group splitting and fission dynamics, to negative effects of how social cues to movement affect disease state [this sentence needs rewording]. We conclude by discussing these results in the context of (sticklebacks-endo parasites), a model system for host-parasite interactions, and outline experimental tests of the model's predictions for social movement and disease transfer.

[to add: actual model predictions, when do it].

Must add references

Results

We form a model that couples disease transmission with both non-social and social influences to movement. In the model, individuals move between a breeding area and a recovery area (Figure 1).

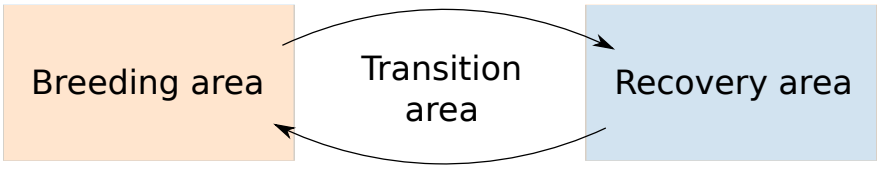

Figure 1: **Model schematic.** The model represents movement between a breeding area, which has high disease transmission and low recovery rates, and a recovery area, which has low disease transmission and high recovery rates.

To analyze the parameter dependence of the model, we consider four "disease transmission regimes", where both recovery and social transmission rate take on high or low values. A high recovery rate means that typical recovery times are similar to to the time needed to move between areas, so that recovery is likely to occur during migration. A high infection rate means that an epidemic can spread through the population before individuals are able to move away from the group or to the recovery area. A low recovery rate means that recovery is unlikely to occur during migration, and that an individual must spend a significant amount of time in the recovery area in order to become healthy once again. A low infection rate means that if individuals change their motion after infection, it is possible to move away from other groupmates before infecting them. Using these definitions, we can define four different disease transfer regimes for each model:

1. **High rates:** High infection rate / High recovery rate
2. **High recovery:** Low infection rate / High recovery rate
3. **High infection:** High infection rate / Low recovery rate
4. **Low rates:** Low infection rate / Low recovery rate

Social influence to motion has a different effect on the fraction infected in each of these cases. With high rates, there are transient epidemics that die quickly, because the infected recover quickly (Fig 2a). Because infection and recovery happen quickly, the group most often stays together as a whole, which often consists of both healthy and infected individuals, and (migratory recovery)

([JD: remember that you wrote summary on page of notebook with blue sticky note]])

In regime 2, low overall infection prevalence

in regime 3, oscillatory infections. There is an epidemic, then the group moves 'together' to the recovery area. Then, move back as recover. At high social though, the group can never split apart, and as a result, recovered individuals don't leave infected individuals while in the recovery area, and then become re-infected. This causes the whole group to essentially stay infected

in regime 4, also oscillatory (?)

The 1D model can capture the mechanisms of what is seen in regimes (3 - only 3??), but not others. This is because the model does not allow realistic group fission. Without noise, there is a fixed threshold at which an individual can break off from the group. In contrast, in the more realistic 2D model, there is randomness

to individual motion, and so there is always a small probability that an individual will break off from the group.

[[or, to address this, should I add noise to the 1D model? An easy way would be to add the noise, but still enforce the positional limits of -1 and 1. Then wouldn't have to deal with drift]]

The 1D model shows that when social weight increases, there can be "transient epidemics" due to social influence to motion. For example, a newly infected individual has a conflicting preference of whether to move to the recovery area or to remain near groupmates, and this causes it to remain by others until enough have become infected that a sub-group reaches consensus to move together to the recovery area. ....Other explanation of 1D model results.... (Figure 2).

Additionally we consider effect of a "reaction time offset", between when an individual becomes infected, and when their personal location preference changes. (Figure 2C).

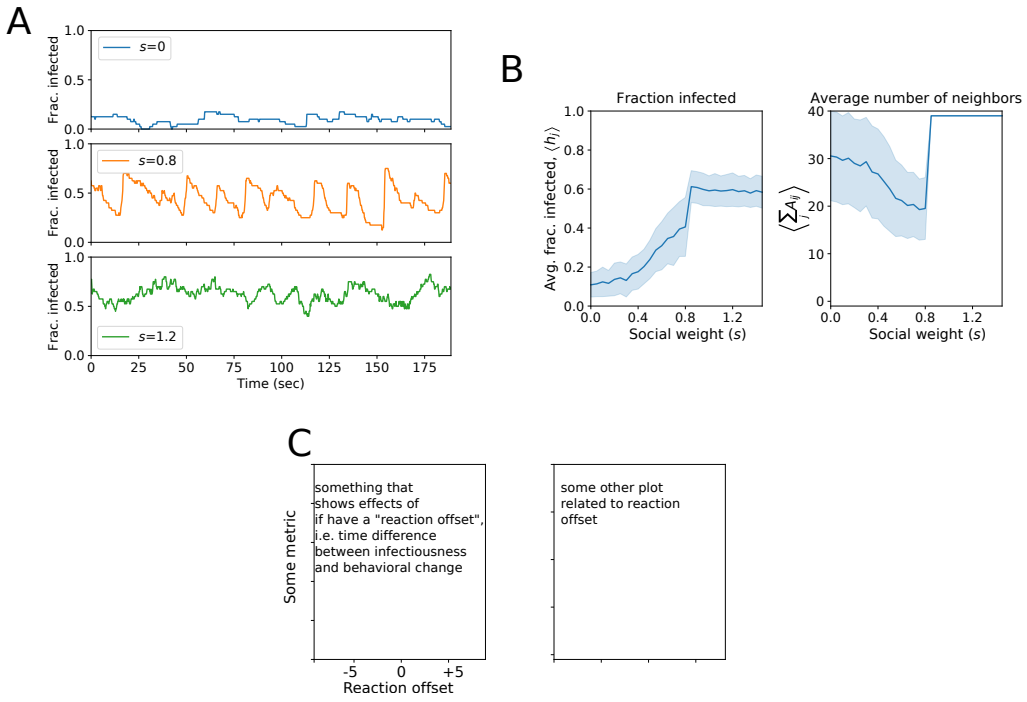

Figure 2: **1D model simulation results.** (A) Time-dependent fraction infected with different values of the social interaction parameter s. (B) Average fraction infected, and average number of neighbors, when social interaction is increased. (C) Something that looks at the effect of have a "reaction offset", i.e. a difference between an individual becomes infected, and when their behavior changes. This could have a negative offset, which means that you are infectious before your personal location preference changes (this will increase disease prevalence). Or it could have a positive offset, which means that you change your personal location preference before you become infectious (this is decrease disease prevalence).

We next use a 2D model with more realistic movement rules. Using these, we see that similarity with results with 1D model, but also some differences because motion is realistic, and groups can undergo fission-fusion

dynamics (Figure 3).

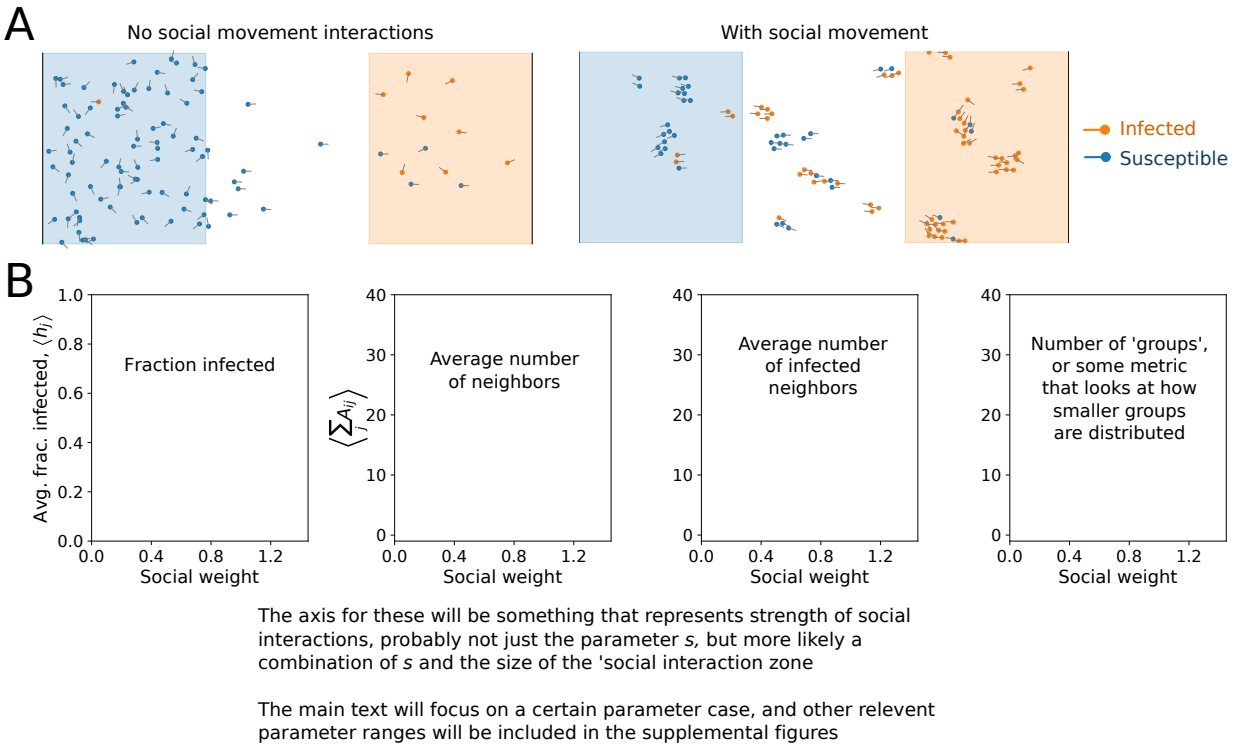

Figure 3: **2D model simulation results.** (A) Illustration of simulation configurations with no social movement interactions, and with with social movement interactions. (B) Average fraction infected, and other quantities, when social interactions vary.

With the 2D model, we ask, what if individuals have different social movement rules that depend on their disease state? We consider the case where healthy individuals can detect infected individuals and respond different to them by [[motion rule that end up changing]] (Figure A). When [[conditions]], the groups separate into "infected" and "healthy" subgroups (Figure B), which decreases overall disease prevalence (Figure C). In this case, also ... (Figure C).

Discussion

Summary of model and results

Discussion topics go here!

Infection and social attraction

Our results suggest that social influences affect both disease prevalence and group movement dynamics. However, infection can also change the degree of gregariousness demonstrated by an individual. For in-

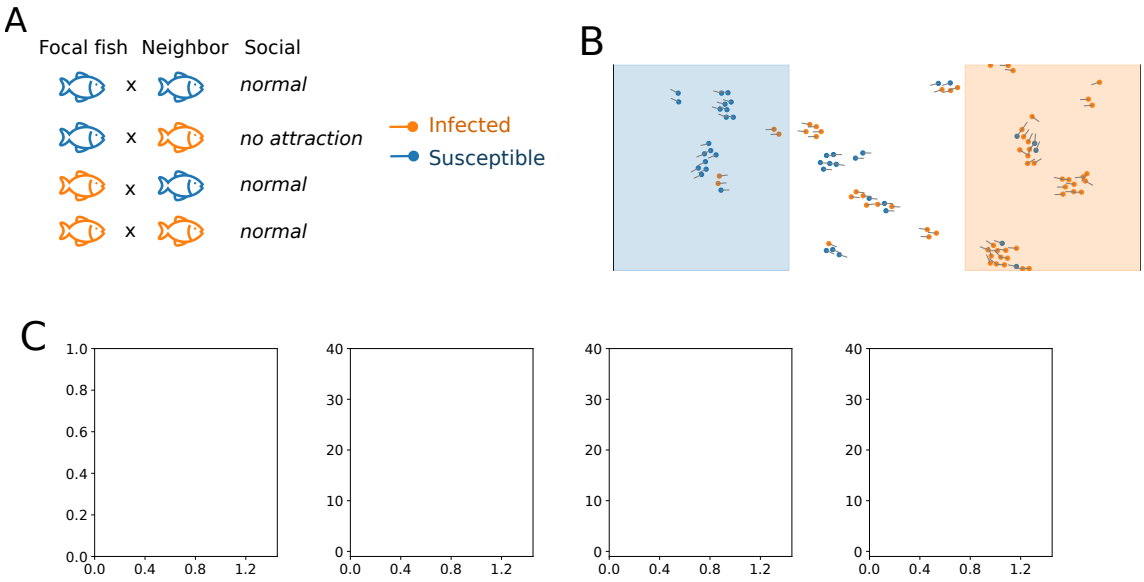

Figure 4: **Social interactions that depend on disease state.** (A) We consider social interactions rules where [[description]]. (B) An example simulation configuration illustrates how fission-fusion movement may separate sub-groups into healthy or infected. (C) The fraction infected decreases... another metric that relates to subgroups.. plots that show these things somehow, after actually doing these simulations.

stance, an immune response triggered during infection can lead to sickness behaviours (Hart 1988): adaptive behavioural changes in infected individuals that help combat infection. This includes anorexia, lethargy, and reduced social interactions. It may be that the social attraction of sick individuals may be quite a bit lower than in healthy, gregarious individuals. This reduced gregariousness has the benefit of reducing disease spread within populations (See Shakhar and Shakhar 2015). Known as the "Eyam hypothesis": sickness behavior protects the social group of infected individuals by limiting their direct contacts, preventing them from contaminating the environment, and broadcasting their health status. Kin selection promotes such behaviors.

Alternatively,

References:

Hart, B.L. 1988 Biological basis of the behavior of sick animals. *Neurosci. Biobehav. Rev.* **12**, 123-137. (doi:https://doi.org/10.1016/S0149-7634(88)80004-6).

Shakhar, K. & Shakhar, G. 2015 Why Do We Feel Sick When Infected—Can Altruism Play a Role? *PLoS Biol* **13**, e1002276. (doi:10.1371/journal.pbio.1002276)

... discussion of systems where this is ecologically relevant. For example, stickleback, as shown in Figure 5. (or some other example).

Discuss, could have evolutionary simulation, for perhaps the social interaction parameters, and simulate to ask what configurations evolve under different environmental pressures.

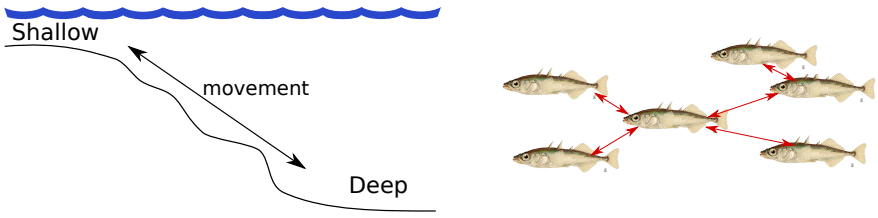

Figure 5: **Ecologically relevant model contexts.** Schooling stickleback fish are a case where social influence to motion is expected to impact the transmission of ecto-parasites (*species name*). In the lake, the fish move between shallow waters, which are used as breeding areas and have higher parasite growth and transmission rates due to the warmer summer temperatures, and deeper waters, which have cooler temperatures and appear to inhibit parasite growth.

Concluding summary and direction of future work.

Methods

Environmental structure

We define three areas which are used to represent movement preferences and disease dynamics. Each of the three areas has a length of $2L$ and is defined using the x-coordinate of position. The breeding area spans $-3L \leq x \leq L$, has high disease transfer and low recovery rates, and is the preferred area for healthy individuals. The transit area spans $-L < x < L$, and has spatially varying disease transfer and recovery rates. The recovery area spans $L \leq x \leq 3L$, has low disease transfer and high recovery rates, and is the preferred area for infected individuals. These three areas are showen in Fig 6A.

We define disease dynamics to vary spatially as defined by a function $T(x)$ for transmission and $R(x)$ for recovery. Individuals can become infected either from the environment (background transmission) or from contact with other individuals (direct transmission). We assume that both forms of transmission are heightened in the breeding area and reduced elsewhere. In contrast, recovery is heightened in the recovery area and reduced elsewhere. We assume that transmission and recovery rates are constant in the breeding and recovery areas, and use a logistic function to describe how both rates change across the transit area:

$$T(x) = \begin{cases} f(L), & \text{if } -3L \leq x \leq -L \text{ (breeding)} \\ f(-x), & \text{if } -L < x < L \text{ (transit)} \\ f(-L), & \text{if } L \leq x \leq 3L \text{ (recovery)} \end{cases} \tag{1}$$

$$R(x) = \begin{cases} f(-L), & \text{if } -3L \leq x \leq -L \text{ (breeding)} \\ f(x), & \text{if } -L < x < L \text{ (transit)} \\ f(L), & \text{if } L \leq x \leq 3L \text{ (recovery)} \end{cases}, \tag{2}$$

where $f(x) = \left(1 + e^{-x/a}\right)^{-1}$ is the logistic function with steepness determined by the parameter a. We consider two different values of a, to represent larger ($a = L/3$) or smaller ($a = L$) changes in rates with movement to the different areas. Fig 6B shows the functions $T(x)$ and $R(x)$ with these two different values.

Movement behavior

We use both a simplified 1D motion model as well as a more realistic 2D model to represent migratory movement between areas. Each model incorporates social influence to movement, disease-dependent personal

location preferences, and location-dependent disease transfer and recovery rates. An agent i has a disease state $h_i = \{0, 1\}$, with 0 representing susceptible (i.e. not infected) and 1 representing infected, and a position x_i (1D model) or $\mathbf{r}_i = (x_i, y_i)$ (2D model).

Non-social location preferences

We define a function $F(x, h)$ to represent personal location preferences that change with the x-coordinate of position (x) and the individual's infection status (h). A susceptible, i.e. healthy, individual ($h = 0$) prefers the breeding area, while an infected individual ($h = 1$) prefers the recovery area. We define a function $F(x, h)$ which represents these disease-dependent location preferences by biasing an individual's movement in the x-direction when outside of the preferred area. We represent this with a piecewise constant form:

$$F(x,h) = \begin{cases} -H(x+L), & \text{if } h = 0 \\ H(-x+L), & \text{if } h = 1 \end{cases}, \tag{3}$$

where $H(\cdot)$ is the Heaviside step function. Thus healthy individuals have a movement bias to the left whenever they are outside of the breeding area and infected individuals have a movement bias to the right whenever they are outside of the recovery area. Fig 6C shows the function $F(x, h)$.

1D model equation of motion

The motion of each agent is described with

$$dx_i = dt \left(\underbrace{\kappa F(x_i, h_i)}_{\text{location preference}} + \underbrace{s \sum_j g\left(x_j - x_i\right)}_{\text{social influence}} \right) \tag{4}$$

The first term represents non-social location preference, with κ as a weighting factor.

The second term represents social information, weighted by s and summed over all individuals. The function $g(\cdot)$ represents that social influences to movement decrease in magnitude with distance, but that within a range individuals adjust their movement towards others. We represent this mathematically with

$$g\left(x_j - x_i\right) = \left(x_j - x_i\right) \exp\left(-\frac{\left(x_j - x_i\right)^2}{2x_0^2} \right), \tag{5}$$

where x_0 is a length scale for how far social interactions extend in space. We use $x_0 = L/10$ for the simulations.

The 1D model represents motion in the transit area between the breeding and recovery areas, but does not capture self-propelled movement or group motion within the the breeding or recovery areas. Additionally, this model cannot represent the effects of having disease-dependent social movement preferences within a given area. To overcome these limitations, we use the 2D model of motion as described below

2D model equation of motion

In the 2D model, susceptible agents in area 1, or infected agents in area 3, only move according to social influences. When outside of the preferred area, an individual moves by weighting both the personal location preference and social influences. To represent motion in a 2D space and allow for group fission-fusion dynamics, we use a modified version of the zonal model of (Couzin et al., 2002; Ioannou et al., 2012b; Couzin

et al., 2005a). An individual swims with a constant speed v, and turning dynamics are given by an equation for angular velocity (Gautrais et al., 2008b):

$$d\omega_i = \frac{1}{\tau}\left(\hat{\mathbf{v}}_i \times \left(\underbrace{\kappa F(x_i, h_i)\hat{x}}_{\text{location preference}} + \underbrace{s\hat{\mathbf{d}}_Z(\{h_j, \mathbf{r}_j, \hat{\mathbf{v}}_j\})}_{\text{social influence}}\right) - \omega\right) dt + \sigma_\omega dW(t), \tag{6}$$

where $\hat{\mathbf{d}}_\mathbf{Z}$ is the desired motion direction from the zonal model, $\hat{x}$ is a unit vector in the x-direction, σ_ω is the noise amplitude, and $W(t)$ is a Wiener process, and an agent i has unit velocity vector $\hat{\mathbf{v}}_i$, position $\mathbf{r}_i = (x_i, y_i)$, and disease state h_i. As in Eq. 4, κ represents the strength of the non-social location preference, and s the strength of social preferences. The non-social location preference depends only on an individual's disease state and x-coordinate of position, while social movement depends on the positions, orientations, and disease states of an agents neighbors. Movement is in the range $-3L \leq x \leq 3L$ and $-L_y \leq y \leq L_y$, with hard boundaries in the x-direction and periodic boundaries in y.

The zonal model represents motion by considering social influence due to discrete 'zones': an outer zone of attraction, a middle zone of alignment, and an inner zone of repulsion. Eq. 6 is a reformulated version of the zonal model in terms of effective torques; we use this in order to simplify how both non-social and social influences combine to determine motion. The desired motion direction in the zonal model is determined as follows: [could add this, or could leave out: how to get d_z. include repulsion, attraction, alignment directions, and also a 'blind spot'. This is the same as described in the other papers, so wouldn't absolutely need this though]. This model has three parameters: r_r is the outer radius for the repulsion zone, r_s is the outer radius for the social zone which includes alignment and attraction, and θ_B defines the blind spot in the back. Fig 6D illustrates these zones.

Eq. 6 is a form of the "persistent-turning-walker" (PTW) model of motion (Gautrais et al., 2008a). We choose parameter value by forming an approximate equivalence between the PTW formulation and the discrete-time formulation of Ioannou et al. (2012a). There, a parameter p was used to weight the zonal model social movement direction versus the current direction, and θ_{max} to represent the maximum turning angle in a given time step, with a value of $dt = 0.1$ used for the time step. To relate these to the social coupling weight s in Eq. 6, consider the case where the zonal model causes turns to be the maximum value θ_{max}. If $\hat{v}_i \times \hat{\mathbf{d}}_\mathbf{Z} \approx 1$, then $s \approx p\theta_{max}/dt \approx 1.6$ radians/sec. Since typically $\hat{v}_i \times \hat{\mathbf{d}}_\mathbf{Z} < 1$, we choose $s = 2$ for approximately equivalent behavior. In the simulations we vary both s and κ.

For the noise amplitude, Ioannou et al. (2012a) added random angles at each time step drawn from a Gaussian distribution with zero mean and standard deviation of approximately $\sigma_m = 0.1$ radians (5.7 degrees) at each time step. Using the fluctuation-dissipation theorem and standard methods of stochastic simulation, we have $var(\sigma_\omega dW(t)) = \sigma_\omega^2 dt = \sigma_m^2$. Plugging in $dt = 0.1$ and $\sigma_m = 0.1$ from Ioannou et al. (2012a), we obtain $\sigma_\omega = \sqrt{(0.1)}$ for equivalence.

We must also choose a value for τ, which represents the time scale for changes in angular velocity (or, equivalently, the turning moment of inertia). In previous simulations of the zonal model, the equation was first order, i.e. neglecting inertia. We therefore choose a small value of $\tau = 0.1$ sec, which means that turns occur on the order of timestep used by Ioannou et al. (2012a).

To define the zonal model parameters, we first set the constant movement speed to $v = 0.02L$. Using the values from Ioannou et al. (2012a), we set the zonal radii to $r_r = 3.657v$ and $r_s = 6.857v$, and additionally use a blind spot of $\theta_B = 0$, for simplicity.

In summary, parameter values are:

Parameter	Value
s	2 (or a range)?
κ	range (?)
τ	0.1 sec.
σ_ω	$\sqrt{0.1}$
v	$0.02L$
r_r	$3.657v$
r_s	$6.857v$
θ_B	0

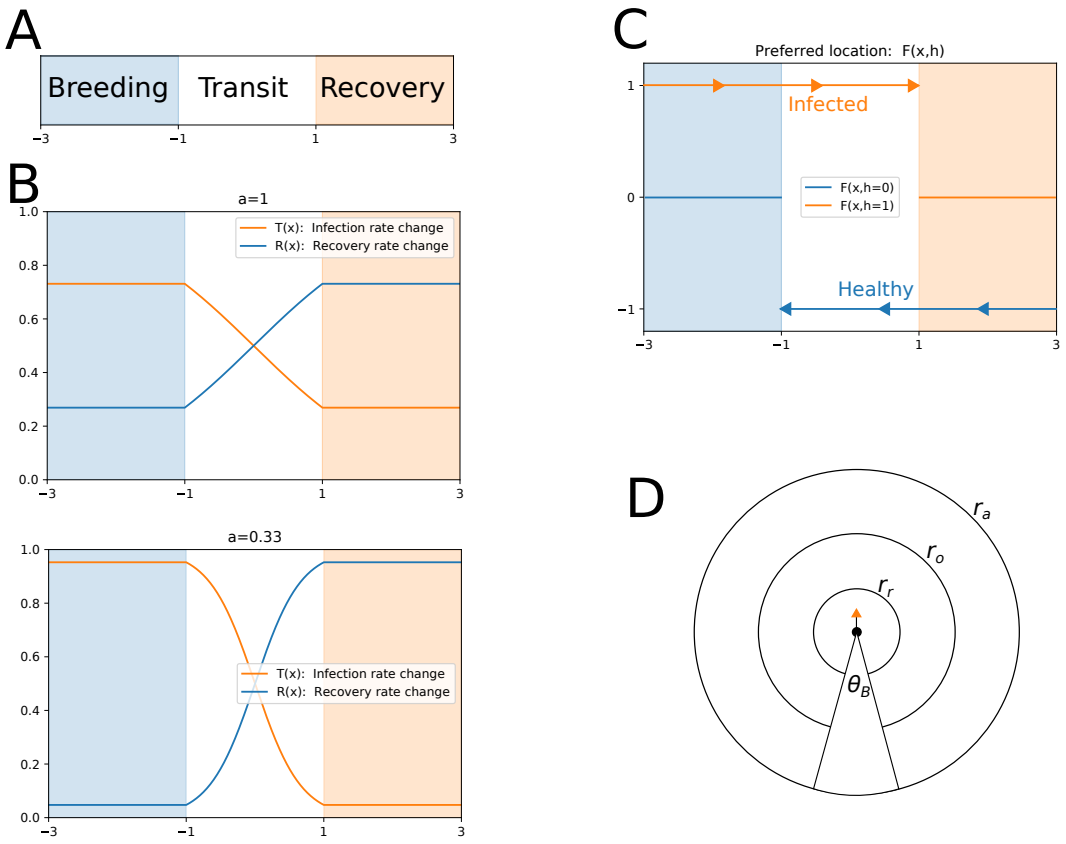

Figure 6: **Model details.** (A) Coordinate system and x-direction limits for the models. (B) Position-dependent infection rates and recovery rates, showing the two different scaling parameters used. (C) Disease-dependent personal location preference, showing arrows for direction of movement bias. (D) **[update figure to just use two zones, outer as r_s]** Illustration of the zonal model used for the 2D simulations, showing the repulsion zone (within r_r), alignment zone (between r_r and r_o), the attraction zone (between r_o and r_a), and the angle defining the blind spot (θ_B).

Infection dynamics

We consider disease transfer and recovery rates that vary with position in the environment as defined by the functions $T(x)$ and $R(x)$ above. We consider that disease transfer occurs between neighbors that are close in space by setting a distance threshold. The distance threshold determines the connections of the time dependent social adjacency matrix, $A_{ij}(t)$, which sets whether or not disease transmission can occur. For

the 1D model, we use the same distance x_0 from Eq. 5 to set the values of the adjacency matrix:

$$A_{ij}^{\mathrm{1D}}(t) = \begin{cases} 1, & \text{if } |x_i(t) - x_j(t)| \leq x_0 \\ 0, & \text{otherwise} \end{cases} \tag{7}$$

For the 2D model, we use the radius of the alignment zone to set the cutoff distance for the social disease transfer adjacency matrix:

$$A_{ij}^{\mathrm{2D}}(t) = \begin{cases} 1, & \text{if } |\mathbf{r}_i(t) - \mathbf{r}_j(t)| \leq r_a \\ 0, & \text{otherwise} \end{cases} . \tag{8}$$

To simulate disease transfer, we consider the SIS model on a network [ref]. Disease transfer between agents is proportional to the rate β, there is a background rate of infection from the environment proportional to the rate α, and recovery rate is proportional to γ. However, since infection and recovery rates also depend on position, and social network weights, the following rules are used to simulate disease transfer during a single timestep of length Δt:

- If agent i is in state $h_i = 0$ (susceptible):
  - Neighbor j transmits disease with probability $\Delta t \beta T(x_i) A_{ij} h_j$
  - Background (environment) infection occurs with probability $\Delta t \alpha T(x_i)$
- If agent i is in state $h_i = 1$ (infected):
  - Recovery occurs with probability $\Delta t \gamma R(x_i)$

This corresponds to the standard SIS model simulated on a network [REFS], modified to account for changes in infection and recovery rates that vary with position.

[NOTE: add somewhere: Although we refer to area on the left as the 'breeding area', breeding and mortality are not explicitly included in the model.].

References

Andrew M. Berdahl, Albert B. Kao, Andrea Flack, Peter A. H. Westley, Edward A. Codling, Iain D. Couzin, Anthony I. Dell, and Dora Biro. Collective animal navigation and migratory culture: from theoretical models to empirical evidence. *Philosophical Transactions of the Royal Society B: Biological Sciences*, 373(1746):20170009, mar 2018. doi: 10.1098/rstb.2017.0009. URL https://doi.org/10.1098%2Frstb.2017.0009.

Iain D. Couzin, Jens Krause, Richard James, Graeme D. Ruxton, and Nigel R. Franks. Collective Memory and Spatial Sorting in Animal Groups. *Journal of Theoretical Biology*, 218(1):1–11, sep 2002. doi: 10.1006/jtbi.2002.3065. URL https://doi.org/10.1006%2Fjtbi.2002.3065.

Iain D. Couzin, Jens Krause, Nigel R. Franks, and Simon A. Levin. Effective leadership and decision-making in animal groups on the move. *Nature*, 433(7025):513–516, feb 2005a. doi: 10.1038/nature03236. URL https://doi.org/10.1038%2Fnature03236.

Iain D. Couzin, Jens Krause, Nigel R. Franks, and Simon A. Levin. Effective leadership and decision-making in animal groups on the move. *Nature*, 433(7025):513–516, feb 2005b. doi: 10.1038/nature03236. URL https://doi.org/10.1038%2Fnature03236.

Jerry B. Covert and William W. Reynolds. Survival value of fever in fish. *Nature*, 267(5606):43–45, may 1977. doi: 10.1038/267043a0. URL https://doi.org/10.1038%2F267043a0.

D. R. Daversa, A. Fenton, A. I. Dell, T. W. J. Garner, and A. Manica. Infections on the move: how transient phases of host movement influence disease spread. *Proceedings of the Royal Society B: Biological Sciences*, 284(1869):20171807, dec 2017. doi: 10.1098/rspb.2017.1807. URL https://doi.org/10.1098%2Frspb.2017.1807.

David R. Daversa, Camino Monsalve-Carcaño, Luis M. Carrascal, and Jaime Bosch. Seasonal migrations body temperature fluctuations, and infection dynamics in adult amphibians. *PeerJ*, 6:e4698, may 2018. doi: 10.7717/peerj.4698. URL https://doi.org/10.7717%2Fpeerj.4698.

Jacques Gautrais, Christian Jost, Marc Soria, Alexandre Campo, Sébastien Motsch, Richard Fournier, Stéphane Blanco, and Guy Theraulaz. Analyzing fish movement as a persistent turning walker. *Journal of Mathematical Biology*, 58(3):429–445, jun 2008a. doi: 10.1007/s00285-008-0198-7. URL https://doi.org/10.1007%2Fs00285-008-0198-7.

Jacques Gautrais, Christian Jost, Marc Soria, Alexandre Campo, Sébastien Motsch, Richard Fournier, Stéphane Blanco, and Guy Theraulaz. Analyzing fish movement as a persistent turning walker. *Journal of Mathematical Biology*, 58(3):429–445, jun 2008b. doi: 10.1007/s00285-008-0198-7. URL https://doi.org/10.1007%2Fs00285-008-0198-7.

V. Guttal and I. D. Couzin. Social interactions information use, and the evolution of collective migration. *Proceedings of the National Academy of Sciences*, 107(37):16172–16177, aug 2010. doi: 10.1073/pnas.1006874107. URL https://doi.org/10.1073%2Fpnas.1006874107.

Richard J. Hall, Sonia Altizer, and Rebecca A. Bartel. Greater migratory propensity in hosts lowers pathogen transmission and impacts. *Journal of Animal Ecology*, 83(5):1068–1077, mar 2014. doi: 10.1111/1365-2656.12204. URL https://doi.org/10.1111%2F1365-2656.12204.

C. C. Ioannou, V. Guttal, and I. D. Couzin. Predatory Fish Select for Coordinated Collective Motion in Virtual Prey. *Science*, 337(6099):1212–1215, aug 2012a. doi: 10.1126/science.1218919. URL https://doi.org/10.1126%2Fscience.1218919.

C. C. Ioannou, V. Guttal, and I. D. Couzin. Predatory Fish Select for Coordinated Collective Motion in Virtual Prey. *Science*, 337(6099):1212–1215, aug 2012b. doi: 10.1126/science.1218919. URL https://doi.org/10.1126%2Fscience.1218919.

Sophie Johns and Allison K. Shaw. Theoretical insight into three disease-related benefits of migration. *Population Ecology*, 58(1):213–221, oct 2015. doi: 10.1007/s10144-015-0518-x. URL https://doi.org/10.1007%2Fs10144-015-0518-x.

M. Kluger, D. Ringler, and M. Anver. Fever and survival. *Science*, 188(4184):166–168, apr 1975. doi: 10.1126/science.1114347. URL https://doi.org/10.1126%2Fscience.1114347.

Ryan S. Mohammed, Michael Reynolds, Joanna James, Chris Williams, Azad Mohammed, Adesh Ramsubhag, Cock van Oosterhout, and Jo Cable. Getting into hot water: sick guppies frequent warmer thermal conditions. *Oecologia*, 181(3):911–917, mar 2016. doi: 10.1007/s00442-016-3598-1. URL https://doi.org/10.1007%2Fs00442-016-3598-1.

Brett R. Moyer and Gary E. Wagenbach. Sunning by Black Noddies (Anous minutus) May Kill Chewing Lice (Quadraceps hopkinsi). *The Auk*, 112(4):1073–1077, oct 1995. doi: 10.2307/4089047. URL https://doi.org/10.2307%2F4089047.

Atle Mysterud, Lars Qviller, Erling L. Meisingset, and Hildegunn Viljugrein. Parasite load and seasonal migration in red deer. *Oecologia*, 180(2):401–407, oct 2015. doi: 10.1007/s00442-015-3465-5. URL https://doi.org/10.1007%2Fs00442-015-3465-5.

Darren Pais and Naomi E. Leonard. Adaptive network dynamics and evolution of leadership in collective migration. *Physica D: Nonlinear Phenomena*, 267:81–93, jan 2014. doi: 10.1016/j.physd.2013.04.014. URL https://doi.org/10.1016%2Fj.physd.2013.04.014.

Alfonso Pérez-Escudero and Gonzalo G. de Polavieja. Collective Animal Behavior from Bayesian Estimation and Probability Matching. *PLoS Computational Biology*, 7(11):e1002282, nov 2011. doi: 10.1371/journal.pcbi.1002282. URL https://doi.org/10.1371%2Fjournal.pcbi.1002282.

Lars Qviller, Nina Risnes-Olsen, Kim Magnus Bærum, Erling L. Meisingset, Leif Egil Loe, Bjørnar Ytrehus, Hildegunn Viljugrein, and Atle Mysterud. Landscape Level Variation in Tick Abundance Relative to Seasonal Migration in Red Deer. *PLoS ONE*, 8(8):e71299, aug 2013. doi: 10.1371/journal.pone.0071299. URL https://doi.org/10.1371%2Fjournal.pone.0071299.

Krzysztof Rakus, Maygane Ronsmans, and Alain Vanderplasschen. Behavioral fever in ectothermic vertebrates. *Developmental & Comparative Immunology*, 66:84–91, jan 2017. doi: 10.1016/j.dci.2016.06.027. URL https://doi.org/10.1016%2Fj.dci.2016.06.027.

William W. Reynolds, Martha E. Casterlin, and Jerry B. Covert. Behavioural fever in teleost fishes. *Nature*, 259(5538):41–42, jan 1976. doi: 10.1038/259041a0. URL https://doi.org/10.1038%2F259041a0.

E Satinoff, G. McEwen, and B. Williams. Behavioral fever in newborn rabbits. *Science*, 193(4258):1139–1140, sep 1976. doi: 10.1126/science.959829. URL https://doi.org/10.1126%2Fscience.959829.

Allison K. Shaw and Sandra A. Binning. Migratory Recovery from Infection as a Selective Pressure for the Evolution of Migration. *The American Naturalist*, 187(4):491–501, apr 2016. doi: 10.1086/685386. URL https://doi.org/10.1086%2F685386.

A. Strandburg-Peshkin, D. R. Farine, I. D. Couzin, and M. C. Crofoot. Shared decision-making drives collective movement in wild baboons. *Science*, 348(6241):1358–1361, jun 2015. doi: 10.1126/science.aaa5099. URL https://doi.org/10.1126%2Fscience.aaa5099.

C. J. Torney, S. A. Levin, and I. D. Couzin. Specialization and evolutionary branching within migratory populations. *Proceedings of the National Academy of Sciences*, 107(47):20394–20399, nov 2010. doi: 10.1073/pnas.1014316107. URL https://doi.org/10.1073%2Fpnas.1014316107.